Eur. Phys. J. A **16**, 63–69 (2003)
DOI 10.1140/epja/i2001-10271-3

THE EUROPEAN PHYSICAL JOURNAL A

Transverse-momentum distribution of J/Ψ's in Pb-Pb collisions and gluon rescattering

P. Zhuang[1,a] and J. Hüfner[2]

[1] Physics Department, Tsinghua University, Beijing 100084, PRC
[2] Institute for Theoretical Physics, University of Heidelberg, D-69120 Heidelberg, Germany

Received: 27 September 2001 / Revised version: 7 July 2002 /
Published online: 17 January 2003 –
Communicated by A. Molinari

Abstract. We study anomalous J/Ψ suppression and $p_{\rm t}$ broadening in the model of prompt gluons. The anomalous suppression can be successfully described in this model. The transverse-momentum dependence of J/Ψ suppression in relativistic heavy-ion collisions is calculated from initial-state gluon rescattering with both nucleons and prompt gluons produced in nucleon-nucleon collisions in the early phase of the reaction. It seems impossible to describe simultaneously anomalous suppression and $p_{\rm t}$ broadening in Pb-Pb collisions within the model of prompt gluons with reasonable values of the parameters.

PACS. 25.75.-q Relativistic heavy-ion collisions – 12.38.Mh Quark-gluon plasma

1 Introduction

Recently, the NA50 Collaboration has presented the final analysis of transverse-momentum distributions [1] for charmonia produced in Pb-Pb collisions at 158 A GeV. For the J/Ψ, the values of $\langle p_{\rm t}\rangle$, $\langle p_{\rm t}^2\rangle$ and $\langle M_{\rm t}-M\rangle$ exhibit a similar trend as a function of the centrality of the collisions: they first increase and then flatten when the centrality increases, and finally turn steeply upward for the most central collisions.

It is commonly accepted [2] that the new data on J/Ψ suppression in Pb-Pb collisions cannot be explained by inelastic collisions of the J/Ψ with the nucleons of projectile and target alone. The anomalous suppression calls for a new absorption mechanism, whose physical origin has not yet been unambiguously identified, however. Among the proposed theories are the deconfinement by a QGP [3, 4], the interactions with comovers [5], the suppression by prompt gluons [6], shadowing in the initial state and many more [2]. We think that a simultaneous description of the data for $\langle p_{\rm t}^2\rangle$ and the suppression may rule out some of these models.

It is generally agreed that the additional transverse-momentum broadening $\delta p_{\rm t}^2 = \langle p_{\rm t}^2\rangle_{AB} - \langle p_{\rm t}^2\rangle_{NN}$ observed in nucleus-nucleus (AB) collisions over the one in nucleon-nucleon (NN) collisions arises in the initial state, *i.e.* before the production of the $c\bar{c}$ pair [7]. The two partons (mostly gluons) traverse nuclear matter thereby colliding with nucleons (thus acquiring additional $p_{\rm t}^2$) before they fuse to the $c\bar{c}$. Indeed, the data for $\langle p_{\rm t}^2\rangle_{AB}$ show a linear relation with the path length of the gluons in the initial state as is well studied in pA and S-U collisions [2]. This behavior of $\delta p_{\rm t}^2$ in pA and S-U collisions will be called normal or Glauber-type broadening, $\langle p_{\rm t}^2\rangle_{\rm G}$.

In a recent publication [8] we have drawn the attention to a close correlation of the values of $\langle p_{\rm t}^2\rangle(E_{\rm t})$ and the degree of anomalous suppression $\Delta S(E_{\rm t}) = S_{\rm G}(E_{\rm t}) - S_{\rm ob}(E_{\rm t})$, where $S_{\rm G}(E_{\rm t})$ (G ="Glauber") is the suppression calculated from the inelastic scattering of the J/Ψ on nucleons alone, while "ob" refers to the observed values. The empirical relation is

$$\langle p_{\rm t}^2\rangle(E_{\rm t}) = \langle p_{\rm t}^2\rangle_{\rm G}(E_{\rm t}) + \frac{\Delta S(E_{\rm t})}{S_{\rm ob}(E_{\rm t})}\delta p_{\rm t}^2 \ . \qquad (1)$$

We call the part, which correlates with ΔS, the anomalous contribution to $\langle p_{\rm t}^2\rangle$. This part must be calculated within the model which reproduces the anomalous suppression ΔS.

In this paper we address the model of prompt gluons or "wounded" nucleons. In the early phase of heavy-ion collisions, nucleons collide with nucleons, they are then excited and become wounded nucleons. A J/Ψ on its way out of the overlap zone of the two nuclei encounters mostly wounded nucleons. These wounded nucleons may cause a strong J/Ψ suppression. In ref. [6], wounded nucleons have been described as nucleons with one or more semihard gluons. Adjusting the mean number of produced prompt gluons in a NN collision, the authors are able to describe the observed anomalous suppression.

[a] e-mail: zhuangpf@mail.singhua.edu.cn

These wounded nucleons (or prompt gluons) should also be present in the initial state. Their presence should also influence the passage of the gluon, which later produces the J/Ψ and should manifest itself in an additional $p_{\rm t}$ broadening.

In our calculation we rely heavily on the notation and on the parameters chosen in ref. [6], yet our presentation is essentially self-contained. In sect. 2 we present the formulas for J/Ψ suppression in Pb-Pb collisions calculated from inelastic J/Ψ N interactions and from collisions with prompt gluons in the final state. Then we turn to the initial state and derive the formulas for the generation of the transverse momentum. Then, in sect. 3, we present the numerical results and compare with experiment, followed by the conclusions in sect. 4.

2 J/Ψ suppression and $\langle p_{\rm t}^2 \rangle$ within the model of prompt gluons

Figure 1 is a schematic representation of J/Ψ production in nucleus-nucleus collisions with particular emphasis to the prompt gluons in the initial and final state. The collision of a row of projectile nucleons on a row of target nucleons is depicted in a two-dimensional (time-longitudinal coordinate) plane and in the NN c.m.s. A gluon from a projectile nucleon and a gluon from a target nucleon fuse to produce a premeson at point O which has three-dimensional space coordinates $(\vec{s}, z_A)$ in the rest frame of the projectile A and $(\vec{b}-\vec{s}, z_B)$ in the rest frame of the target B, where $\vec{b}$ is the impact parameter for the AB collision. The premeson propagates through the projectile and the target, and develops in time towards the asymptotically observed J/Ψ. During the propagation the premeson interacts with nucleons from the projectile and target. Since these nucleons have experienced collisions with other nucleons before their encounter with the $c\bar{c}$ premeson, and since they have radiated bremsstrahl "prompt" gluons (dashed lines), the $c\bar{c}$ premeson will also interact with these radiated gluons. Taking into account the two kinds of final-state collisions of the premeson, the J/Ψ suppression function can be written as

$$S(E_{\rm t}) = \int {\rm d}^2\vec{b}{\rm d}^2\vec{s}{\rm d}z_A{\rm d}z_B K(\vec{b},\vec{s},z_A,z_B,E_{\rm t}) \ , \qquad (2)$$

where $E_{\rm t}$ is the transverse energy which reflects the centrality of the collision, and the expression for the suppression kernel K is taken as [6]

$$K(\vec{b},\vec{s},z_A,z_B,E_{\rm t}) = \rho_A(\vec{s},z_A)\rho_B(\vec{b}-\vec{s},z_B)e^{-(I_A+I_B)}P(E_{\rm t}|b) \ . \qquad (3)$$

Here $\rho_{A,B}(\vec{r})$ is the density of the nuclei A and B, respectively. The final-state J/Ψ absorption via the interaction with nucleons and prompt gluons in the geometric row labeled by the variables $\vec{b},\vec{s}$ is contained in the two

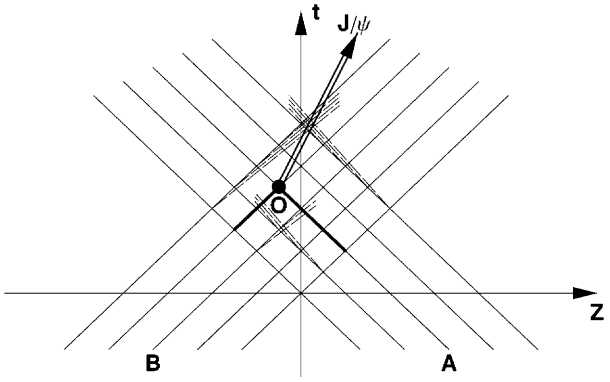

Fig. 1. A two-dimensional (time-longitudinal coordinate) plot for J/Ψ production in a collision of nuclei A and B in the c.m.s. of the colliding nucleons. Nucleons are denoted by thin solid lines, the two gluons which fuse to form a premeson at point O are denoted by thick solid lines, while the bremsstrahl gluons are drawn by dashed lines.

exponentials given by

$$\begin{aligned} I_A(\vec{b},\vec{s},z_A,z_B) &= \int_{z_A}^{\infty} {\rm d}z\sigma_{\rm abs}^{\Psi N}(t_\Psi)\rho_A(\vec{s},z) \\ &\quad + \sigma_{\rm in}^{NN}\int_{z_A}^{\infty}{\rm d}z\int_{-\infty}^{\infty}{\rm d}z'\sigma_{\rm abs}^{\Psi g}(t_\Psi)\Theta(t_g) \\ &\quad \times\langle n_g\rangle(t_g)\rho_A(\vec{s},z)\rho_B(\vec{s}-\vec{b},z') \ , \\ I_B(\vec{b},\vec{s},z_A,z_B) &= \int_{-\infty}^{z_B} {\rm d}z\sigma_{\rm abs}^{\Psi N}(t_\Psi)\rho_B(\vec{s}-\vec{b},z_B) \\ &\quad + \sigma_{\rm in}^{NN}\int_{-\infty}^{z_B}{\rm d}z\int_{-\infty}^{\infty}{\rm d}z'\sigma_{\rm abs}^{\Psi g}(t_\Psi)\Theta(t_g) \\ &\quad \times\langle n_g\rangle(t_g)\rho_B(\vec{s}-\vec{b},z)\rho_A(\vec{s},z') \ , \end{aligned} \qquad (4)$$

where $\sigma_{\rm in}^{NN}$ is the inelastic NN cross-section, $\langle n_g\rangle$ is the mean number of prompt gluons produced in a NN collision, and $\sigma_{\rm abs}^{\Psi N}$ and $\sigma_{\rm abs}^{\Psi g}$ are the J/Ψ absorption cross sections for its interaction with a nucleon and with a prompt gluon, respectively. Effects of formation time for the development of a $c\bar{c}$ pair to the J/Ψ and for the radiation of a gluon are taken care of by the time dependence of $\sigma_{\rm abs}^{\Psi N}(t_\Psi)$ and $\langle n_g\rangle(t_g)$, respectively. Here t_Ψ is the time difference between the ΨN interaction point and the formation point O of the premeson, and t_g is the time difference between the Ψg interaction point and the NN interaction point which produces the prompt gluon. The Θ-functions in I_A and I_B ensure that only the prompt gluons, which are created before the interaction with the effective J/Ψ, are taken into account.

Using the two-channel model for the evolution of a $c\bar{c}$ pair, the time dependent effective cross-section $\sigma_{\rm abs}^{\Psi N}$ can be expressed as [9]

$$\sigma_{\rm abs}^{\Psi N}(\tau) = \sigma_{\rm in}^{\Psi N} + (\sigma_{\rm in}^{\rm pre} - \sigma_{\rm in}^{\Psi N})\cos(\Delta M\tau) \ , \qquad (5)$$

where $\sigma_{\rm in}^{\rm pre}$ is the premeson and $\sigma_{\rm in}^{\Psi N}$ the J/Ψ absorption cross-section, and ΔM is the mass difference between J/Ψ

and Ψ'. We use values $\sigma_{\rm in}^{\Psi N} = 6.7\,{\rm mb}$ and $\sigma_{\rm in}^{\rm pre} = 3\,{\rm mb}$ [6]. While $\sigma_{\rm abs}^{\Psi N}$ oscillates in the proper time, after the integration over the collision geometry the absorption increases monotonously with the increasing centrality.

In the constituent quark model, the inelastic Ψg cross-section differs from the inelastic ΨN cross-section by a factor 3/4 [6],

$$\sigma_{\rm abs}^{\Psi g} = \frac{3}{4}\sigma_{\rm abs}^{\Psi N} \ . \tag{6}$$

Within pQCD the time dependence of the mean number $\langle n_g\rangle$ of the radiated gluons can be calculated [6] with an adjustable parameter $\omega_{\rm min}$, the soft limit of the transverse momentum carried by the prompt gluons. In order to reduce the numerical efforts, it is parameterized [6] as a step function

$$\langle n_g\rangle(t_g) = \begin{cases} n_g^0\ \frac{t_g}{t_0}, & t_g < t_0\ , \\ n_g^0, & t_g > t_0\ . \end{cases} \tag{7}$$

In our numerical calculations we have used fixed values [6] $t_0 = 0.6\,{\rm fm}/c$ and $n_g^0 = 0.75$ (corresponding to $\omega_{\rm min} = 0.75$ GeV) for Pb-Pb collisions at 158 A GeV.

To include the effect of transverse-energy fluctuations which have been shown to be significant for the explanation of the sharp J/Ψ suppression in the domain of very large $E_{\rm t}$ values, we relate the mean number $\langle n_g\rangle$ to the transverse energy in the same way as the energy density [10] and the comover density [5],

$$\langle n_g\rangle \to \langle n_g\rangle \frac{E_{\rm t}}{\langle E_{\rm t}\rangle(b)}\ , \tag{8}$$

where the mean value $\langle E_{\rm t}\rangle(b)$ is proportional to the number of participant nucleons at fixed b, $\langle E_{\rm t}\rangle(b) = qN_p(b)$, and $N_p(b)$ is determined by the collision geometry. The function $P(E_{\rm t}|b)$ in the suppression kernel (3) describes the distribution of transverse energy in events at a given impact parameter b. It is chosen as a Gaussian distribution [10]

$$P(E_{\rm t}|b) = \frac{1}{\sqrt{2\pi q^2 a N_p(b)}} e^{-\frac{(E_{\rm t}-\langle E_{\rm t}\rangle(b))^2}{2q^2 a N_p(b)}} \tag{9}$$

with the parameters $q = 0.274$ GeV and $a = 1.27$ [10].

We now turn to calculate the J/Ψ transverse momentum within the mechanism of gluon rescattering in the initial state. Before the two gluons, one from the projectile and one from the target, fuse to form the $c\bar{c}$ premeson at point O, either of them may scatter off one or several nucleons and one or several prompt gluons, as shown in fig. 1. Via the exchange of transverse momentum at each interaction vertex, the mean-squared transverse momentum of the J/Ψ is a function of the history of the two gluons,

$$\langle p_{\rm t}^2\rangle(\vec{b},\vec{s},z_A,z_B) = \langle p_{\rm t}^2\rangle_{NN} + \frac{\langle p_{\rm t}^2\rangle_{gN}}{\lambda_{gN}}\ell_{gN}(\vec{b},\vec{s},z_A,z_B) + \frac{\langle p_{\rm t}^2\rangle_{gg}}{\lambda_{NN}\lambda_{gg}}\ell_{gg}^2(\vec{b},\vec{s},z_A,z_B)\ . \tag{10}$$

Here the first term is the contribution from the $c\bar{c}$ production vertex in an isolated NN collision, while the second and third terms arise, respectively, from multiple gN and gg collisions before fusion. Since the number of the gN collisions is proportional to the number of nucleons which the two gluons encounter, the second term scales with the sum of the lengths of the two gluon paths,

$$\ell_{gN}(\vec{b},\vec{s},z_A,z_B) = \int_{-\infty}^{z_A} {\rm d}z\rho_A(\vec{s},z)/\rho_0 + \int_{z_B}^{\infty} {\rm d}z\rho_B(\vec{s}-\vec{b},z)/\rho_0\ . \tag{11}$$

The constant before the length ℓ_{gN} in eq. (10) depends on the mean transverse momentum $\langle p_{\rm t}^2\rangle_{gN}$ acquired in a gN collision and on the mean free path λ_{gN} of a gluon in nuclear matter. The third term in eq. (10) is proportional to the number of NN collisions in which the prompt gluons are generated. Therefore, ℓ_{gg}^2 is a sum of two 2-dimensional integrations (similar to the second terms in I_A and I_B in the final-state interaction),

$$\ell_{gg}^2(\vec{b},\vec{s},z_A,z_B) = \int_{z_B}^{\infty}{\rm d}z\int_{-\infty}^{z_A}{\rm d}z'\langle n_g\rangle(t_g) \times\rho_A(\vec{s},z)\rho_B(\vec{s}-\vec{b},z')/\rho_0^2 + \int_{-\infty}^{z_A}{\rm d}z\int_{z_B}^{\infty}{\rm d}z'\langle n_g\rangle(t_g) \times\rho_B(\vec{s}-\vec{b},z)\rho_A(\vec{s},z')/\rho_0^2\ . \tag{12}$$

The other factors in the last term of eq. (10) are: The mean free path $\lambda_{NN}^{-1} = \rho_0\sigma_{NN}^{\rm in}$ for inelastic NN scatterings (the source of the prompt gluons) and $\lambda_{gg}^{-1} = \rho_g\sigma_{gg}$ the mean free path for the interaction of a gluon (which fuses to form the $c\bar{c}$) with a prompt gluon. We use $\sigma_{\rm in}^{NN} = 32\,{\rm mb}$ and $\rho_0 = 0.17/\,{\rm fm}^3$, while $\langle p_{\rm t}^2\rangle_{gg}/\lambda_{gg}$ is considered as a free parameter. The effect of transverse-energy fluctuations can also be included in the initial state interaction by making the transformation (8) for the mean number $\langle n_g\rangle$ of the prompt gluons, like in the final-state interaction.

We will call ℓ_{gg}^2 the squared gluon length related to gg interactions. However, it is necessary to note that while ℓ_{gN} is a geometrical length, either term in ℓ_{gg}^2 is not a simply product of the two geometrical lengths, since production time effects of the prompt gluons are included via the mean number $\langle n_g\rangle$.

The expression (10) for the mean transverse momentum holds for a J/Ψ produced from the rows with coordinates $\vec{b},\vec{s},z_A$ and z_B. In order to compare with the experimental data, we have to average. The average of a quantity $Q(\vec{b},\vec{s},z_A,z_B)$ at fixed transverse energy $E_{\rm t}$ is calculated from the suppression kernel K (eq. (3))

$$\langle Q\rangle(E_{\rm t}) = \int {\rm d}^2\vec{b}{\rm d}^2\vec{s}{\rm d}z_A{\rm d}z_B\, Q(\vec{b},\vec{s},z_A,z_B) \times K(\vec{b},\vec{s},z_A,z_B,E_{\rm t})/S(E_{\rm t})\ . \tag{13}$$

Inserting expression eq. (10) into eq. (13), one obtains

$$\langle p_{\rm t}^2\rangle(E_{\rm t}) = \langle p_{\rm t}^2\rangle_{NN} + \frac{\langle p_{\rm t}^2\rangle_{gN}}{\lambda_{gN}}\langle \ell_{gN}\rangle(E_{\rm t}) + \frac{\langle p_{\rm t}^2\rangle_{gg}}{\lambda_{NN}\lambda_{gg}}\langle \ell_{gg}^2\rangle(E_{\rm t}) = \langle p_{\rm t}^2\rangle_{NN} + \frac{\langle p_{\rm t}^2\rangle_{gN}}{\lambda_{gN}}\langle \ell_{gN}^{\rm eff}\rangle(E_{\rm t}) \ , \quad (14)$$

where we have introduced the effective gluon length $\langle \ell_{gN}^{\rm eff}\rangle$ in nuclear matter defined by

$$\langle \ell_{gN}^{\rm eff}\rangle(E_{\rm t}) = \langle \ell_{gN}\rangle(E_{\rm t}) + \frac{\langle p_{\rm t}^2\rangle_{gg}/(\lambda_{NN}\lambda_{gg})}{\langle p_{\rm t}^2\rangle_{gN}/\lambda_{gN}}\langle \ell_{gg}^2\rangle(E_{\rm t}) \ . \quad (15)$$

3 Results

To simplify the numerical calculations we use a constant nuclear density $\rho(r) = \rho_0\Theta(R_A - r)$. This is certainly a crude approximation and can be improved upon whether the model promises success. Since the calculation of the average transverse momentum needs information of the suppression function $S(E_{\rm t})$, we first calculate the ratio of the J/Ψ to Drell-Yan cross-sections $\sigma_\Psi(E_{\rm t})/\sigma_{\rm DY}(E_{\rm t}) = S_\Psi(E_{\rm t})/S_{\rm DY}(E_{\rm t})$. Here S_Ψ is the J/Ψ suppression function eq. (2), and the Drell-Yan cross-section $S_{\rm DY}$ is obtained by putting $I_A = I_B = 0$ in the kernel K of S. The results are shown in fig. 2 as a function of $E_{\rm t}$ together with the new data of the NA50 Collaboration. The calculation is normalized at $E_{\rm t} = 0$ (NN collision) to $\sigma_\Psi/\sigma_{\rm DY} = 50$. In the absence of the Gaussian distribution in $E_{\rm t}$ (eq. (9)) and its fluctuations related to $\langle n_g\rangle$ (eq. (8)), we have the same results as in [6]. It is obvious that the final-state interaction with only nucleons (dashed line) cannot reproduce the data. The results including final-state interactions with prompt gluons (thin solid line) fit the $E_{\rm t}$-dependence well, except for the fast drop at very large $E_{\rm t}$ values. According to refs. [10,5], the drop at high $E_{\rm t}$ arises from transverse-energy fluctuations. Including the $E_{\rm t}$ fluctuations via eq. (8) the agreement with data is improved, but less than the data seem to require. The quality of the fit is about as good as in ref. [5] and the residual discrepancy in the agreement with data may have its origin in the $E_{\rm t}$ assignment (c.f. ref. [5]).

The average gluon lengths (eq. (15)) are plotted in fig. 3 as a function of $E_{\rm t}$. The length $\langle \ell_{gN}\rangle$ in nuclear matter (dashed line) and the length $\sqrt{\langle \ell_{gg}^2\rangle}$ related to prompt-gluon contribution but without consideration of transverse-energy fluctuations (thin solid line) have the same behavior and almost the same amplitude. They increase in the domain of small transverse energies ($E_{\rm t} < 50$ GeV), and then saturate with $E_{\rm t}$ for values $E_{\rm t} > 50$ GeV, where one observes large anomalous suppression and the prompt gluons become important. The saturation of the gluon lengths and of the transverse momentum (shown below) in this domain is due to the saturation of the amount

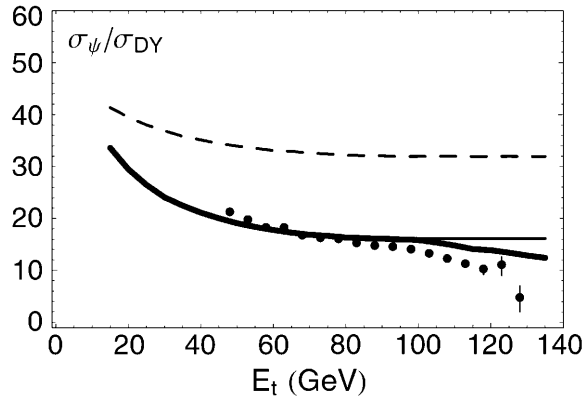

Fig. 2. The relative J/Ψ production cross-section $\sigma_\Psi/\sigma_{\rm DY}$ in Pb-Pb collisions at 158 A GeV [11] as a function of transverse energy. The dashed line corresponds to the normal nuclear suppression, the thin solid line is obtained with final-state rescattering with nucleons and prompt gluons, and the thick solid line is calculated including the fluctuations in transverse energy.

of matter traversed by the initial gluons in the Pb-Pb collisions. As for the suppression in fig. 2, the contribution of the transverse-energy fluctuations is significant only for very high transverse energies, $E_{\rm t} > 100$ GeV (solid line in fig. 3).

The effects of initial gN and gg scattering to the average transverse momentum are controlled by the two parameters, $\langle p_{\rm t}^2\rangle_{gN}/\lambda_{gN}$ and $\langle p_{\rm t}^2\rangle_{gg}/\lambda_{gg}$, respectively. The former may be extracted from experiments with light projectiles, and the latter is determined from the fit of eq. (10) to the data in the $E_{\rm t}$ region where prompt gluons become important. With the isolated NN contribution $\langle p_{\rm t}^2\rangle_{NN} = 1.11$ $({\rm GeV}/c)^2$ and the gN contribution $\langle p_{\rm t}^2\rangle_{gN}/\lambda_{gN} = 0.081$ $({\rm GeV}/c)^2/{\rm fm}$ [1], the transverse momentum calculated with only gN scattering (dashed line in fig. 4), namely considering only the first two terms in eq. (10), agrees well with the data in the domain of $E_{\rm t} < 50$ GeV, while it is clearly below the data outside this domain. Including the initial scattering with prompt gluons but without the factor eq. (8) (thin solid line) and choosing the parameter $\langle p_{\rm t}^2\rangle_{gg}/\lambda_{gg} = 1/35\ \langle p_{\rm t}^2\rangle_{gN}/\lambda_{gN}$, satisfactory agreement is obtained for all the data except for the last point, where the transverse-energy fluctuations are expected to play a crucial rule. We include the fluctuations in $E_{\rm t}$ via the factor eq. (8) which becomes relevant only for ℓ_{gg}^2 in eq. (10) and arrive at the solid line in fig. 4. There is some improvement, but the significance is difficult to judge, since there is only one data point with rather large error bar.

In order to see the results of our calculations in a different form, we display the experimental and calculated values for $\langle p_{\rm t}^2\rangle(E_{\rm t})$ as a function of $\langle \ell_{gN}\rangle(E_{\rm t})$, fig. 5a, and as a function of $\langle \ell_{gN}^{\rm eff}\rangle(E_{\rm t})$ (eq. (15)), fig. 5b. While the dependence $\langle p_{\rm t}^2\rangle$ *versus* $E_{\rm t}$ is rather complicated with strong saturation effects for large values of $E_{\rm t}$, the dependence $\langle p_{\rm t}^2\rangle$ *versus* $\langle \ell_{gN}\rangle$ or $\langle \ell_{gN}^{\rm eff}\rangle$ is nearly a straight line. The dashed and solid lines in figs. 5a,b correspond to the theo-

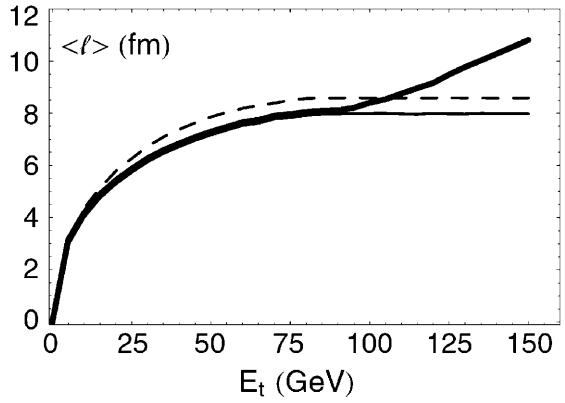

Fig. 3. The gluon lengths $\langle \ell_{gN} \rangle$ (dashed line) and $\sqrt{\langle \ell_{gg}^2 \rangle}$ without (thin solid line) and with (thick solid line) fluctuations in transverse energy as a function of the transverse energy.

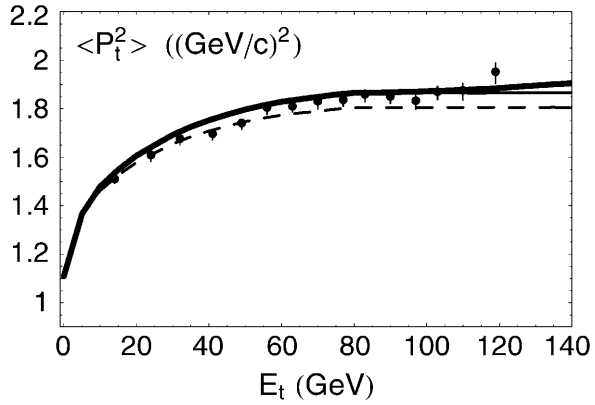

Fig. 4. The average squared transverse momentum $\langle p_{\rm t}^2 \rangle$ as a function of transverse energy. The data are from [1]. The dashed line corresponds to the normal gluon rescattering on nucleons, the thin solid line is obtained with gluon rescattering with nucleons and prompt gluons, and the thick solid line is calculated with also the fluctuations in transverse energy.

retical curves in fig. 4. According to the definition eq. (14), the slopes of the two straight lines are the same and equal to $\langle p_{\rm t}^2 \rangle / \lambda_{gN} = 0.081$ (GeV/c)^2/ fm.

Until now, we have studied the behavior of $\langle p_{\rm t}^2 \rangle$ as a function of $E_{\rm t}$. In the experiment under consideration [1] the authors have also measured the $p_{\rm t}$ distributions within a given $E_{\rm t}$ interval. They have displayed their data as a ratio

$$R_{i/1}(p_{\rm t}) = \frac{S(p_{\rm t}|E_{\rm t}^{(i)})}{S(p_{\rm t}|E_{\rm t}^{(1)})}\,, \tag{16}$$

where $S(p_{\rm t}|E_{\rm t}^{(i)})$ is the differential distribution in $p_{\rm t}$, normalized to $\int {\rm d}^2 p_{\rm t}\, S(p_{\rm t}|E_{\rm t}^{(i)}) = S(E_{\rm t}^{(i)})$. We have calculated $S(p_{\rm t}|E_{\rm t}^{(i)})$ by assuming a Gaussian $p_{\rm t}$-dependence. Then the suppression function $S(p_{\rm t}|E_{\rm t}^{(i)})$ can be written

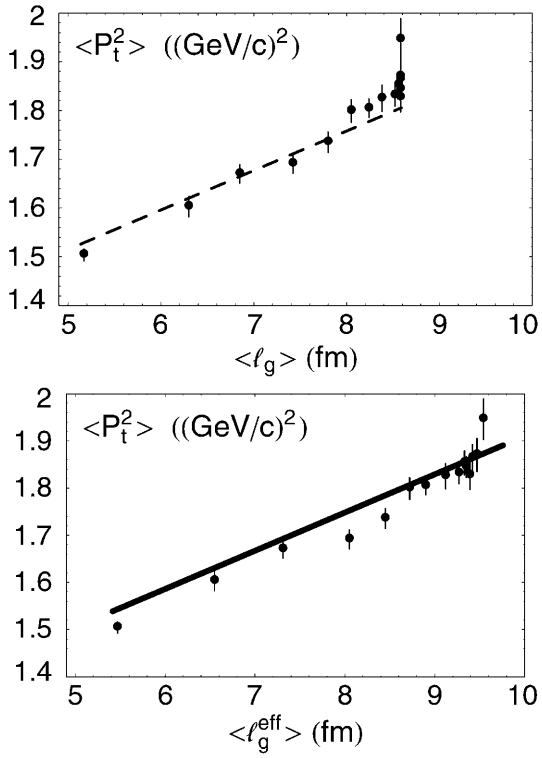

Fig. 5. The observed $\langle p_{\rm t}^2 \rangle (E_{\rm t})$ plotted *versus* the calculated $\langle \ell_{gN} \rangle$ and $\langle \ell_{gN}^{\rm eff} \rangle$. The data are from [1].

as

$$S(p_{\rm t}|E_{\rm t}^{(i)}) = \int {\rm d}^2\vec{b}{\rm d}^2\vec{s}{\rm d}z_A{\rm d}z_B K(\vec{b},\vec{s},z_A,z_B,E_{\rm t}^{(i)}) \times \frac{1}{\langle p_{\rm t}^2\rangle(\vec{b},\vec{s},z_A,z_B)} e^{-\frac{p_{\rm t}^2}{\langle p_{\rm t}^2\rangle(\vec{b},\vec{s},z_A,z_B)}}\,. \tag{17}$$

For the comparison with the experimental data, we divide the $E_{\rm t}$ region into five bins with mean values $E_{\rm t} =$ 23, 48, 70, 90, 110. The theoretical results together with the data are shown in fig. 6.

For the figures we have not followed ref. [1], who plot $R_{i/1}$ *versus* $p_{\rm t}$, but we rather plot $\ln R_{i/1}$ *versus* $\Delta M = \sqrt{M^2 + p_{\rm t}^2} - M$. This representation leads to a straight line for the data integrated over $E_{\rm t}$ (cf. [1]). According to figs. 6, this representation also leads to nearly straight lines. The solid lines represent our calculations. For all ratios, except $R_{5/1}$, the data are well accounted for. We see a problem in the quantity $R_{5/1}$. Our prediction is consistently below the data, although our integrated value $S(E_{\rm t}^{(5)})$ with $E_{\rm t}^{(5)} = 110$ GeV lies *above* the data (fig. 2). Thus, we would have expected our calculation to be consistently above. In order to see whether calculated and experimental slopes agree, we have normalized the calculated curve at small $p_{\rm t}$ to the data. The renormalized result is shown by the upper line and describes the data reasonably well, though there may be systematic deviations at large $p_{\rm t}$. But since the error bars are too large, speculations about the discrepancies may be dangerous.

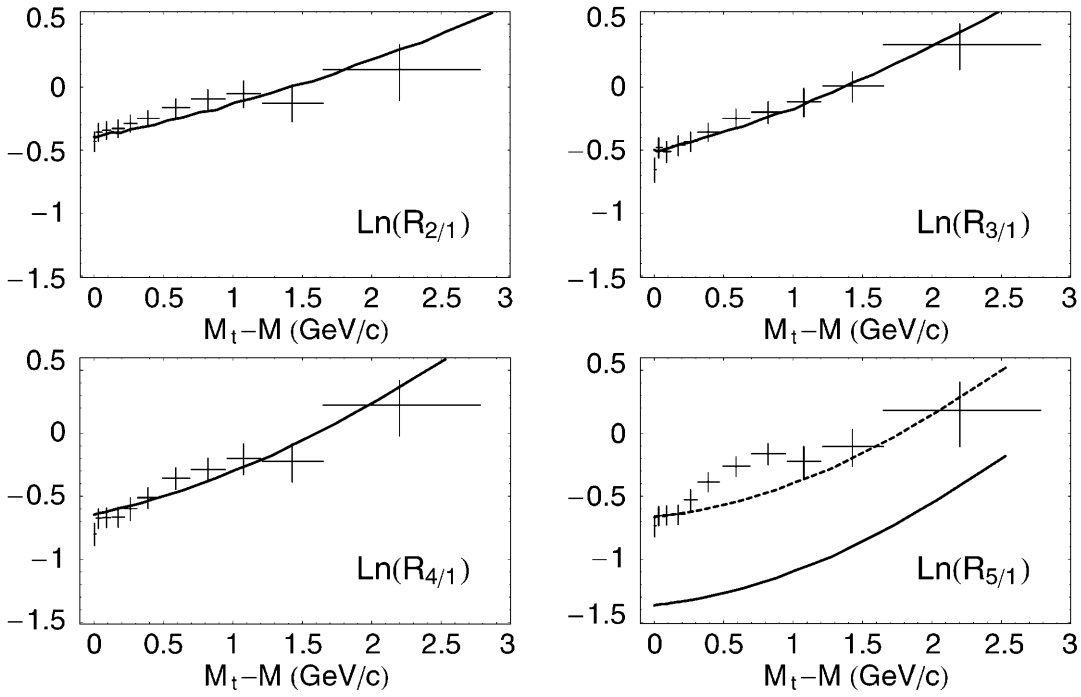

Fig. 6. The ratio $R_{i/1}$ of the J/Ψ cross-section with large value $E_{\rm t}^{(i)}$ in the $E_{\rm t}$ bin i to the cross-section with small $E_{\rm t}^{(1)}$ in the first $E_{\rm t}$ bin as a function of $M_{\rm t} - M$. We have plotted the logarithm of this quantity, since the global data seem to be exponentials $\exp(-(M_{\rm t} - M)/T)$. There are five $E_{\rm t}$ bins corresponding to mean $E_{\rm t} = 23,\ 48,\ 70,\ 90,\ 110$ GeV. The data are from [1]. The theoretical lines are calculated with initial and final-state rescattering with nucleons and prompt gluons and with transverse-energy fluctuations. For $R_{5/1}$, the lower line is our calculation, while the upper line represents the calculated curve normalized to the data for small $M_{\rm t} - M$.

4 Conclusions

In this paper, we have studied the transverse-momentum dependence of J/Ψ production in Pb-Pb collisions at 158 A GeV. We have investigated the mechanism of prompt gluons for both effects, anomalous suppression of J/Ψ and anomalous values of $\langle p_{\rm t}^2 \rangle$. Here, "anomalous" is judged with respect to the "conventional" values of suppression and $\langle p_{\rm t}^2 \rangle$ derived from the data of pA and S-U collisions. The conventional physics is shown as dashed lines in figs. 2 and 4, while the anomaly is the difference between the data and these lines. While the anomaly is large (an effect of a factor 2) in the suppression data, fig. 2, the anomaly is small for the values of $\langle p_{\rm t}^2 \rangle$. The difference between the data and the dashed line is less than 10%, if we use $\langle p_{\rm t}^2 \rangle_{AB} - \langle p_{\rm t}^2 \rangle_{\rm G}$ as the baseline. Within the model of prompt gluons we describe the data for the J/Ψ suppression (except possibly at very high values of $E_{\rm t}$) by introducing one adjustable parameter, the number of produced hard prompt gluons per NN collision (eq. (7)),

$$n_g^0 = 0.75 \ . \tag{18}$$

Within the same model we describe also the data for $\langle p_{\rm t}^2 \rangle$, fig. 4, after a new parameter

$$\left(\frac{\langle p_{\rm t}^2 \rangle_{gg}}{\lambda_{gg}} \right) \Big/ \left(\frac{\langle p_{\rm t}^2 \rangle_{gN}}{\lambda_{gN}} \right) = \frac{1}{35} \tag{19}$$

is adjusted. The magnitude of the values, eqs. (18) and (19), for the two parameters reflects the observation that the anomaly in the suppression is large (50%) while it is a small effect for the values of $\langle p_{\rm t}^2 \rangle$.

Are the extracted values of these two parameters consistent? We discuss the problem in the following way. The mean free paths for the interactions of a gluon which fuses to form the J/Ψ with a nucleon and with a prompt gluon are $\lambda_{gN} = 1/\rho_0 \sigma_{gN}$ and $\lambda_{gg} = 1/\rho_g \sigma_{gg}$, respectively. The density of prompt gluons, ρ_g, is the product of the nucleon density with the average number of inelastic collisions and the prompt gluon number n_g. On the average, a nucleon experiences about 3 collisions in a central Pb-Pb collision. Therefore, we estimate $\rho_g = 3\rho_0 n_g^0$. Substituting the mean free paths into (19), we have

$$n_g^0 \sim \frac{1}{35} \frac{\langle p_{\rm t}^2 \rangle_{gN} \sigma_{gN}}{3 \langle p_{\rm t}^2 \rangle_{gg} \sigma_{gg}} \ . \tag{20}$$

In the constituent quark model, the cross-section σ_{gN} is about 3 times the cross-section σ_{gg}. Assuming that the mean transverse momentums obtained from the two kinds of interactions are about equal at the energy of interest, we extract

$$n_g^0 \sim \frac{1}{35} \ , \tag{21}$$

which is much smaller than the value extracted from the anomalous suppression (18). This means that the two fit parameters (18) and (19) are inconsistent with each other.

We thank Boris Kopeliovich who drew our attention to the initial-state interactions. We are grateful to our referee, who forced us to seriously face the inconsistency between eqs. (18) and (21), which had been originally hidden and whose comments led us to revise our conclusions. One of the authors (P.Z.) is grateful for the hospitality at the Institute for Theoretical Physics in Heidelberg, his work was supported by the grants 06HD954, NSFC19925519 and G2000077407.

References

1. NA50 Collaboration (M.C. Abreu *et al.*), Phys. Lett. B **499**, 85 (2001).
2. R. Vogt, Phys. Rep. **310**, 197 (1999); C. Gerschel, J. Hüfner, Annu. Rev. Nucl. Part. Sci. **49**, 255 (1999).
3. T. Matsui, H. Satz, Phys. Lett. B **178**, 416 (1986).
4. J.P. Blaizot, J.Y. Ollitrault, Phys. Rev. Lett. **77**, 1703 (1996); C.Y. Wong, Phys. Rev. C **55**, 2621 (1997); D. Kharzeev *et al.*, Z. Phys. C **74**, 307 (1997).
5. A. Capella, E.J. Feireiro, A.B. Kaidalov, Phys. Rev. Lett. **85**, 2080 (2000); A. Capella. A.B. Kaidalov, D. Sousa, nucl-th/0105021.
6. J. Hüfner, B.Z. Kopeliovich, Phys. Lett. B **445**, 223 (1998); J. Hüfner, Y.B. He, B.Z. Kopeliovich, Eur. Phys. J. A **7**, 239 (2000).
7. S. Gavin, M. Gyulassy, Phys. Lett. B **214**, 241 (1988); J. Hüfner, Y. Kurihara, H.J. Pirner, Phys. Lett. B **215**, 218 (1988); J. P. Blaizot, J. Y. Ollitrault, Phys. Lett. B **217**, 392 (1989).
8. J. Hüfner, P. Zhuang, Phys. Lett. B **515**, 115 (2001).
9. J. Hüfner, B.Z. Kopeliovich, Phys. Rev. Lett. **76**, 192 (1996).
10. J.P. Blaizot, P.M. Dinh, J.Y. Ollitrault, Phys. Rev. Lett. 85, 4010 (2000).
11. NA50 Collaboration (M.C. Abreu *et al.*), Phys. Lett. B **449**, 128 (1999).